Entropy Effect on Physical Displacement of Redox Molecules in a Nafion Film as Studied by Double Potential-Step Chronoabsorptometry

Masayuki Yagi,*,†,‡ Masahiko Takahashi,§ Masahiro Teraguchi,‡,§ Takashi Kaneko,‡,§ and Toshiki Aoki‡,§

Faculty of Education and Human Sciences, Niigata University, 8050 Ikarashi-2, Niigata 950-2181, Japan, Faculty of Engineering, Niigata University, 8050 Ikarashi-2, Niigata 950-2181, Japan, and Center for Transdisciplinary Research, Niigata University, 8050 Ikarashi-2, Niigata 950-2181, Japan

Received: July 23, 2003

Charge transport (CT) in a Nafion film incorporating $[(NH_3)_5Ru(\mu\text{-pz})Ru(NH_3)_5]^{4+}$ ($[Ru^{II}-Ru^{II}]^{4+}$; pz = pyrazine) was studied using a double potential-step chronoabsorptometry (DPSCA) technique. The oxidative CT by $[Ru^{II}-Ru^{II}]^{4+}/[Ru^{II}-Ru^{III}]^{5+}$ (in a potential step from −0.2 to 0.3 V; first step) was compared with that by $[Ru^{II}-Ru^{III}]^{5+}/[Ru^{III}-Ru^{III}]^{6+}$ (in a successive potential step from 0.3 to 0.7 V; second step). The predominant CTs by a physical displacement mechanism of the complexes were suggested for both of the steps. However, the rate constant of the CT for the first step was 5.2 time higher than that for the second step at 25 °C. The results on CT kinetics and dynamics revealed that the CTs in both of the steps are entropy-controlled in the activation at room temperature. The $\Delta H^{\ddagger}$ (12 kJ mol^{-1}) for the physical displacement in the second step was lower than that (24 kJ mol^{-1}) for the first step, showing that the physical displacement for the second step is enthalpically favorable compared with that for the first step. The corresponding $\Delta S^{\ddagger}$ (−234 J K^{-1} mol^{-1}) for the second step is lower than that ($\Delta S^{\ddagger} = -184$ J K^{-1} mol^{-1}) for the first step, making the physical displacement for the second step more entropically difficult than that for the first step. The entropy effect on the physical displacement was discussed on the basis of the interaction of the complexes with Nafion and reorganization of the solvent (water) molecule involved in the process. The $\Delta S^{\ddagger}$ for the physical displacement of redox complexes in the film decreased with the positive charge of the complexes, suggesting that the highly positive-charged complex is entropically unfavorable for physical displacement, presumably due to higher degree of solvation of the complex and the sulfonate groups in their dissociation.

Introduction

The wide range of promising applications of polymer-modified electrodes[1,2] in the field of electroanalysis,[2] electrocatalysis,[3−6] photoelectrochemistry,[7] and solar energy conversion[8,9] has given impetus to develop these kinds of electrodes. The elucidation of the nature of charge transport (CT) in electroactive polymer films is one of the most interesting fundamental subject in the field, as well as a question of practical importance for the development of new electrode systems, because CT in the films is a key process for the films to work efficiently in most case. Lots of trailblazing great works on the nature of CT in the polymer films have been reported.[10−20] However, ambiguous issues on the mechanism still remain.

Our attentions have been focused on the understanding of a CT mechanism and its controlling factors in nonconductive polymer films incorporating functional redox molecules. In such films, charges are transported by a physical displacement mechanism of the redox molecules and/or by a charge hopping mechanism between them. We have reported analyses of the CT mechanism in Nafion films containing some kinds of redox molecules.[21−25] These works provided the activation parameters for each mechanism, affording a clue to evaluate the controlling factors of CT. The activation parameters for a charge hopping mechanism were nearly explained by the features of the self-exchange reaction of the redox pair. On the other hand, what is responsible for activation parameters for a physical displacement mechanism remained insufficiently resolved.To elucidate activation parameters for a physical displacement mechanism, we designed a $[(NH_3)_5Ru(\mu\text{-pz})Ru(NH_3)_5]^{4+}$ ($[Ru^{II}-Ru^{II}]^{4+}$; pz = pyrazine)/Nafion film system. $[Ru^{II}-Ru^{II}]^{4+}$is known to undergo 1-electron oxidation to $[Ru^{II}-Ru^{III}]^{5+}$ at 0.13 V vs SCE in an aqueous solution, and the formed $[Ru^{II}-Ru^{III}]^{5+}$ doing further 1-electron oxidation to $[Ru^{III}-Ru^{III}]^{6+}$ at 0.52 V. [26,27] The two steps of reversible oxidation enables us to compare the CT by $[Ru^{II}-Ru^{II}]^{4+}/[Ru^{II}-Ru^{III}]^{5+}$ and that by $[Ru^{II}-Ru^{III}]^{5+}/[Ru^{III}-Ru^{III}]^{6+}$ in the film using a double-potential-step technique. This comparison could reveal the influence of charge of the complexes on the CT in the film. Herein, we report the analysis of two steps of the CT in the $[Ru^{II}-Ru^{II}]^{4+}$/Nafion film as studied by double potential-step chronoabsorptometry (DPSCA), and the predominant CT was found to be by a physical displacement mechanism. The entropy effect on CT by the physical displacement of a redox molecule in a polymer film will be first discussed.

Experiments

Materials. Pentaamminechlororuthenium(III) chloride was purchased from Aldrich Chemical Co. Inc. and used as received. The purest grade of silver(I) trifluoroacetate (Kanto Kagaku)

* To whom correspondence should be addressed. Tel & Fax: +81-25-262-7151. E-mail: yagi@ed.niigata-u.ac.jp.
† Faculty of Education and Human Sciences.
‡ Center for Transdisciplinary Research.
§ Faculty of Engineering.

10.1021/jp036146c CCC: $25.00
Published on Web 10/17/2003

and ammonium hexafluorophosphate (Wako Pure Chemical Industries, Ltd.) were used without further purification. Nafion 117 solution (5 wt % alcoholic solution) was purchased from Aldrich Chemical Co. Inc., and diluted to 2.5 wt % with methanol before use.

Preparation. *[$(NH_3)_5Ru(\mu\text{-}pz)Ru(NH_3)_5$]$(PF_6)_4$ ([$Ru^{II}-Ru^{II}$]-$(PF_6)_4$).* [$Ru^{II}-Ru^{II}$]$(PF_6)_4$ was prepared by the modified method of Creutz and Taube.[26] To 0.2 g (0.69 mmol) of pentaamminechlororuthenium(III) chloride suspension in 0.6 mL of water was added 0.29 g (1.3 mmol) of silver(I) trifluoroacetate. It was dissolved on a hot plate at 80 °C before silver chloride was coagulated, and then it was filtered. The filtrate was kept under argon overnight after adding several pieces of freshly prepared amalgamated zinc and 0.027 g (0.34 mmol) of pyrazine. Zinc amalgam was removed by filtration under the argon atmosphere to yield the purple solution. A saturated aqueous solution of ammonium hexafluorophosphate was slowly added to the solution to give a purple deposit. It was collected by filtration after cooling to 0 °C and washed with ethanol. The solid was recrystallized from hot water under argon, yielding 0.15 g of purple needle crystals (42% yield). The product was characterized by UV−visible absorption and IR spectra.

Nafion Film Incorporating [$Ru^{II}-Ru^{II}$]$^{4+}$. A Nafion film was prepared by casting a 2.5 wt % Nafion solution (10 μL) onto an indium tin oxide (ITO) electrode (area 1 cm^2; 10 Ω/□) and air-drying. The film thickness was calculated as 1.0 μm using the volume (10 μL) and density (0.83 g cm^{-3}) of the Nafion solution cast, the density (2.0 g cm^{-3}) [14] of the Nafion film, and the electrode area (1.0 cm^2).[28] A Nafion-coated ITO electrode incorporating [$Ru^{II}-Ru^{II}$]$^{4+}$ (ITO/Nf-[$Ru^{II}-Ru^{II}$]$^{4+}$) was prepared by adsorbing [$Ru^{II}-Ru^{II}$]$^{4+}$ from its aqueous solution into the Nafion film. The amount of the complex incorporated into the film was varied by changing the dipping time or concentration (0.5−5 mM) of the complex solution, and it was quantified from the visible absorption spectral change of the aqueous solution (λ_{max} = 547 nm, ϵ = 30 000 M^{-1} cm^{-1}) before and after the adsorption. The absorbance change was more than 25% relative to the absorbance before the adsorption in all film preparations. The complex concentration in the film was obtained from its amount in the film and the film volume.

Measurements. DPSCA measurements were carried out by combining a photodiode array spectrophotometer (Shimadzu, Multispec-1500) with an electrochemical analyzer (Hokuto Denko, HZ-3000). A conventional single-compartment spectrophotometric cell was equipped with a modified working electrode, a saturated calomel reference electrode (SCE), and a platinum wire counter electrode. The supporting electrolyte solution of 0.1 M KNO_3 (pH = 6.8) was deaerated by bubbling argon gas for ca. 30 min before the measurements.

Results and Discussion

A cyclic voltammogram (CV) of [$Ru^{II}-Ru^{II}$]$^{4+}$ in an aqueous solution exhibited two reversible redox waves at 0.13 and 0.50 V vs SCE as shown in Figure 1a. These are consistent with data (0.13 and 0.52 V vs SCE) reported by Creutz and assigned to the redox responses of [$Ru^{II}-Ru^{II}$]$^{4+}$/[$Ru^{II}-Ru^{III}$]$^{5+}$ and [$Ru^{II}-Ru^{III}$]$^{5+}$/[$Ru^{III}-Ru^{III}$]$^{6+}$, respectively.[26] In a CV of ITO/Nf-[$Ru^{II}-Ru^{II}$]$^{4+}$ dipped in an aqueous electrolyte solution (Figure 1b), the corresponding reversible redox waves were also gained at similar potentials (0.09 and 0.46 V), and the same assignment as the CV in the solution was reasonably applied to these redox waves. It is worth remarking that the charge amount (513 μC cm^{-2}) passed in the first oxidative wave at 0.09 V is much larger than that (147 μC cm^{-2}) in the second one at 0.46 V, in contrast to the close charge amount passed between the first and second waves on the CV in the solution (89.5 and 105 μC cm^{-2} for the first and second waves, respectively). The CV data in Figure 1a suggests that in the solution system the electrochemical reaction including electron transfer between the redox species and the electrode and its diffusion in the solution is not so different in kineticics between the first and second redox processes. In the Nafion film system, however, the kineticics of the electrochemical reaction is distinguishably deferent between the first and second redox process. This could be ascribed to the different CT in the film between the first and second redox processes because the peak separation of each redox wave is similar to that in the corresponding wave in the solution suggesting the similar electron-transfer rates of [$Ru^{II}-Ru^{II}$]$^{4+}$ and [$Ru^{II}-Ru^{III}$]$^{5+}$ with the ITO electrode.

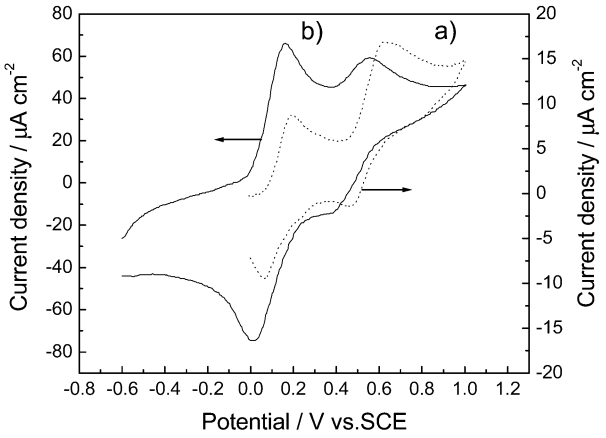

Figure 1. Cyclic voltammograms of (a) an aqueous solution containing 1 mM [$Ru^{II}-Ru^{II}$]$^{4+}$ and 0.1 M KNO_3, and (b) an ITO/Nf-[$Ru^{II}-Ru^{II}$]$^{4+}$ dipped in an aqueous 0.1 M KNO_3 solution. The scan rate is 20 mV s^{-1} for the CVs.

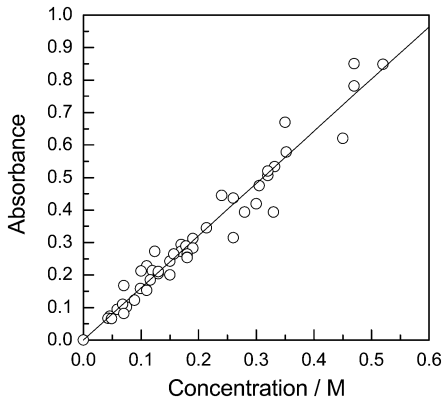

Figure 2. Plots of absorbance at 537 nm of Nf-[$Ru^{II}-Ru^{II}$]$^{4+}$ vs complex concentration in the film.

Electrospectrophotometric techniques are useful in following the direct change of the redox molecule that is responsible to CT in a film, and it is more advanced relative to the conventional electrochemical techniques in that respect. To investigate the CT in the Nf-[$Ru^{II}-Ru^{II}$]$^{4+}$ film using an electrospectrophotometric technique, we first measured the absorption spectrum of the film. The spectrum showed the absorption maximum at λ_{max} = 537 nm, and the absorbance at 537 nm linearly increased with the complex concentration as shown in Figure 2. This linear relationship corroborates the homogeneities of the confined complex and the film thickness. The slope of the straight line gave a molar absorption coefficient (ϵ = 16 100 ± 300 M^{-1} cm^{-1}) of [$Ru^{II}-Ru^{II}$]$^{4+}$ in the film. Figure 3 shows the

TABLE 1: Summary of Absorption and Redox Properties of $[(NH_3)_5Ru(\mu\text{-}O)Ru(NH_3)_5]^{n+}$ in Aqueous Solution and Nafion Film

	λ_{max} (ϵ/$M^{-1}cm^{-1}$)			$E_{1/2}$/V vs SCE[a]	
system	$Ru^{II}-R^{II}$	$Ru^{II}-R^{III}$	$Ru^{III}-R^{III}$	$Ru^{II}-R^{II}/Ru^{II}-R^{III}$	$Ru^{II}-R^{III}/Ru^{III}-R^{III}$
aqueous solution	547 (30 000)	565 (21 000)[b]	352 (6100)[b]	0.13	0.50
Nafion membrane	537 (16 100)	552 (12 200)	no absorption peak in a visible region (>400 nm)	0.09	0.46

[a] Measured in a 0.1 M KNO_3 medium. [b] Reference 27.

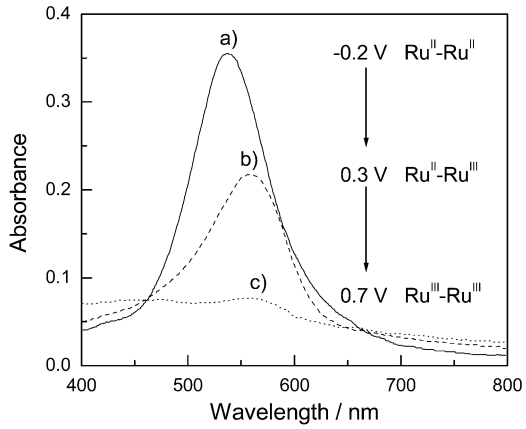

Figure 3. Absorption spectra of ITO/Nf-$[Ru^{II}-Ru^{II}]^{4+}$ dipped in 0.1 M KNO_3 aqueous solution after applying potential of (a) −0.2, (b) +0.3, and (c) +0.7 V vs SCE. The complex concentration in the film is 0.22 M.

absorption spectra of the film after applying the potential of −0.2, 0.3, and 0.7 V for a few minutes. Spectrum (a) at −0.2 V is identical to that before applying the potential. The applied potentials of 0.3 and 0.7 V provided the spectra (b) and (c), respectively, both of which are assigned to those of $[Ru^{II}-Ru^{III}]^{5+}$ and $[Ru^{III}-Ru^{III}]^{6+}$ in the film. Spectrum (b) for $[Ru^{II}-Ru^{III}]^{5+}$ (at 0.3 V) showed the absorption maximum at λ_{max} = 552 nm, and the absorbances at 552 nm versus the complex concentration also gave a straight line. The molar absorption coefficient (ϵ/M^{-1} cm^{-1}) of $[Ru^{II}-Ru^{III}]^{5+}$ in the film was obtained to be 12 200 M^{-1} cm^{-1} (at 552 nm) from the slope of the line. In spectrum (c) for $[Ru^{III}-Ru^{III}]^{6+}$ (at 0.7 V), the distinguishable absorption peak was not observed in the visible region (>400 nm). The back step of the potential from 0.7 to −0.2 V recovered more than 90% of the absorbance before applying the potential for all of the potential step experiments employed. The values of λ_{max} and ϵ for each redox species were summarized in Table 1 together with electrochemical data. λ_{max} shifted to a shorter wavelength for all three species in the Nafion film, and ϵ decreased for at least $[Ru^{II}-Ru^{II}]^{4+}$ and $[Ru^{II}-Ru^{III}]^{5+}$. Curtis reported the considerable solvatochromism of the dπ → π* metal-to-ligand charge transfer (MLCT) band of $[Ru(NH_3)_5pz]^{2+}$.[29] The MLCT band energy decreased with the increase in solvent donor number. This was explained by the net effect of the hydrogen bond between the ammine ligands and solvents increasing the electron density on the Ru center to raise the Ru dπ level. $[Ru^{II}-Ru^{II}]^{4+}$ also showed a similar solvatochromism with a lower energy shift in a higher donor number solvent. On the basis of the reports by Curtis and this result, the blue shift of the MLCT band of $[Ru^{II}-Ru^{II}]^{4+}$ in the Nafion film could suggest dehydration of the complex by electrostatic interaction with the sulfonate groups of Nafion.

An example of a time course of the absorbance at λ_{max} = 537 nm of ITO/Nf-$[Ru^{II}-Ru^{II}]^{4+}$ in potential-step chronoabsorptometry from −0.2 to +0.3 V (first step) is shown in

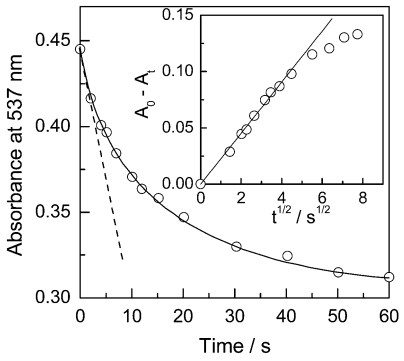

Figure 4. Absorbance change at 537 nm with time in potential-step chronoabsorptometry from −0.2 to 0.3 V vs SCE. Inset shows plots of $A_0 - A_t$ vs $t^{1/2}$ according to eq 1. The complex concentration in the film is 0.26 M.

Figure 4. The apparent diffusion coefficient for D_{app} (cm^2 s^{-1}) in the film can be obtained from the absorbance decrease using the modified Cottrell eq 1

$$A_0 - A_t = 2c_0(\epsilon_{II,II} - \epsilon_{II,III})(D_{app}t/\pi)^{1/2} \quad (1)$$

where A_0 and A_t are the absorbances at 537 nm of the film at time zero and t, respectively, c_0 (M) is the initial concentration of $[Ru^{II}-Ru^{II}]^{4+}$ in the film, $\epsilon_{II,II}$ and $\epsilon_{II,III}$ (M^{-1} cm^{-1}) are the molar absorption coefficients at 537 nm of $[Ru^{II}-Ru^{II}]^{4+}$ and $[Ru^{II}-Ru^{III}]^{5+}$, respectively, and t(s) is reaction time. $\epsilon_{II,II}$ is 16 100 M^{-1} cm^{-1} (vide supra), and $\epsilon_{II,III}$ was obtained to be 9600 M^{-1} cm^{-1} from the slope of the linear plots of the absorbance in saturation of its decrease versus c_0. The plots of $A_0 - A_t$ vs $t^{1/2}$ according to eq 1 gave a linear relationship up to 87% completion of the reaction (30 s) shown in the inset of Figure 4, and the slope of the line gave $D_{app} = 1.3 \times 10^{-10}$ cm^2 s^{-1} (at c_0 = 0.26 M) for the first step. The successive potential-step chronoabsorptometry from 0.3 to 0.7 V yielded $D_{app} = 1.0 \times 10^{-11}$ cm^2 s^{-1} (at c_0 = 0.26 M) for the second redox in a similar manner.

We have reported that analyses of the initial CT rate [30] (v_{CT}/M s^{-1}) are of use to investigate the CT mechanism.[21-25,31] The v_{CT} was defined as eq 2 and approximately estimated from the tangent of the initial absorbance change (537 nm) at time zero as shown by a dot line in Figure 4

$$v_{CT} = \frac{\{d(A_0 - A_t)/dt\}_{initial}}{(\epsilon_{II,II} - \epsilon_{II,III})L} \quad (2)$$

where L is the film thickness (1.0 μm). The plots of v_{CT} versus c_0 for the first and second steps gave the linear relationships at each temperature as shown in Figure 5, parts A and B, respectively, indicating unimolecular CT process with respect to the redox molecule for both the steps.

There are two possible CT mechanisms in a nonconductive polymer incorporating redox molecules: (1) physical displacement of the molecules and (2) charge hopping between the

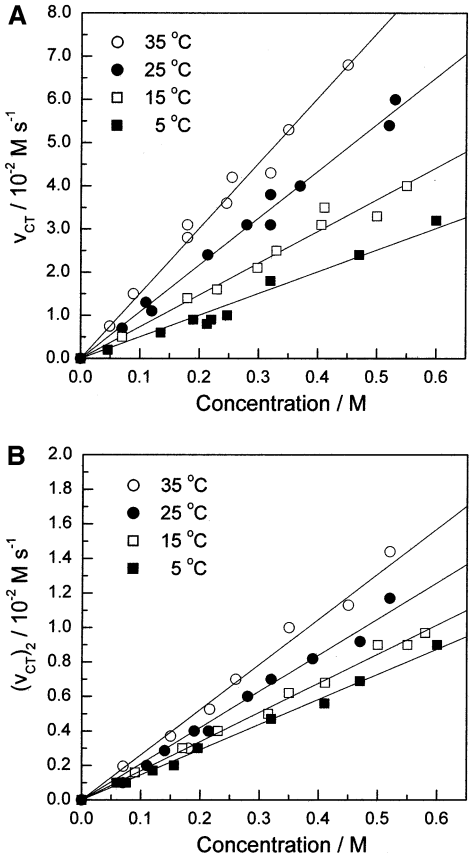

Figure 5. Plots of initial CT rate (v_{CT}/M s^{-1}) vs complex concentration for various temperature for the first step (A) and second step (B); 35 °C, (○); 25 °C, (●); 15 °C, (□); 5 °C, (■).

TABLE 2: Summary of $(k_p)_1$ and $(k_p)_2$ Values

temperature/°C	$(k_p)_1/10^{-2}$ s^{-1}	$(k_p)_2/10^{-2}$ s^{-1}
5	5.0 ± 0.2	1.5 ± 0.02
15	7.4 ± 0.2	1.7 ± 0.02
25	10.9 ± 0.2	2.1 ± 0.04
35	15.1 ± 0.3	2.6 ± 0.09

molecules. The CT by physical displacement of the redox molecules in the film is treated as a unimolecular process because it is based on its physical diffusion, though it involves diffusions of both the oxidized and reduced species of the redox couple. On the other hand, the CT by charge hopping that is based on self-exchange electron transfer between the redox couple should be a bimolecular process. When the CT takes place by both physical displacement and charge hopping, the v_{CT} can be represented by eq 3 which is a combination of first-order physical displacement and second-order charge hopping:[21−25,31]

$$v_{CT} = k_p c_0 + k_c c_0^2 \quad (3)$$

where k_p (s^{-1}) and k_c (M^{-1} s^{-1}) are the first-order rate constant for CT by physical displacement and the second-order rate constant by charge hopping, respectively. The linear relationships on the v_{CT} vs c_0 plots in Figure 5, parts A and B, suggest a physical displacement mechanism at each temperature for both the step. The slopes of the lines yielded the k_p values[32] that were summarized in Table 2. The k_p for the first step, $(k_p)_1$, is 5.2 times larger than $(k_p)_2$ for the second step at 25 °C. The $(k_p)_1$ increased by 3.0 times with the temperature increase from 5 to 35 °C, with $(k_p)_2$ increasing by 1.7 times with the same temperature change.

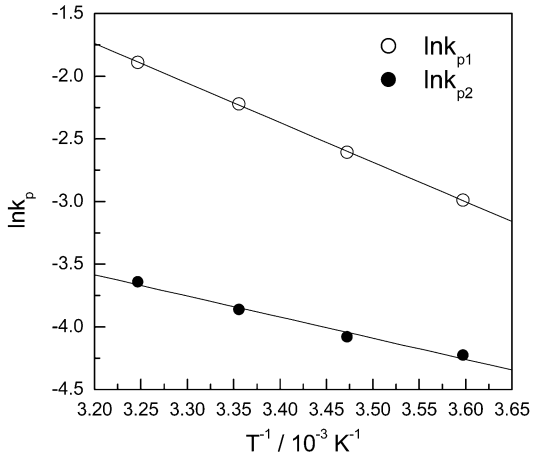

Figure 6. Arrhenius plots of first-order rate constant (k_p/s^{-1}) of the physical displacement for the first step (○) and second step (●). *T*/K is the absolute temperature.

The physical displacement for both the first and second steps involves an activation processes as shown by the linear Arrhenius plots for $(k_p)_1$ and $(k_p)_2$ in Figure 6, the slopes of the lines giving the activation energies (E_a/kJ mol^{-1}). E_a (26 ± 0.3 kJ mol^{-1}) for the physical displacement in the first step is higher than that (E_a = 14 ± 1.2 kJ mol^{-1}) for the second step. The activation energies and other activation parameters at 25 °C for each step were summarized in Table 3. $\Delta G^{\ddagger}$ (79 kJ mol^{-1}) for the first step was slightly lower than that (83 kJ mol^{-1}) for the second step although E_a for the first step is higher than that for the second step. The positive $\Delta H^{\ddagger}$ and negative $\Delta S^{\ddagger}$ were obtained for both the steps. The lower $\Delta H^{\ddagger}$ (12 kJ mol^{-1}) for the second step than that ($\Delta H^{\ddagger}$ = 24 kJ mol^{-1}) for the first step indicates that the physical displacement for the second step is enthalpically favorable compared with that for the first step, whereas the corresponding $\Delta S^{\ddagger}$ (−234 J K^{-1} mol^{-1}) for the second step is lower than that ($\Delta S^{\ddagger}$ = −184 J K^{-1} mol^{-1}) for the first step, making the physical displacement for the second step more entropically difficult than that for the first step. The entropic factor overcomes the corresponding enthalpic one, providing the lower $(k_p)_2$ than $(k_p)_1$ at room temperature. The value of $-T\Delta S^{\ddagger}$ is much higher than $\Delta H^{\ddagger}$ value for each step at 25 °C, showing that the physical displacement are entropy-controlled at a room temperature for both the steps. However, the fractions ($-T\Delta S^{\ddagger}/\Delta G^{\ddagger}$ = 89%) of entropic contribution at 25 °C for the second step are higher than that (70%) for the first step.

In the present system where the cationic complex is electrostatically attached to the anionic sulfonate groups of Nafion, a physical displacement mechanism should require the dissociation of the complexes from the sulfonate groups involving reorganization of the solvent (water), as shown in Figure 7, which is responsible for the positive $\Delta H^{\ddagger}$ and negative $\Delta S^{\ddagger}$ for the physical displacement. The positive $\Delta H^{\ddagger}$ could be explained by a summation of endothermic dissociation enthalpy of the cationic complex from the sulfonate groups and exothermic interactions of the complex and the sulfonate groups with water molecules in the solvent reorganization. The lower $\Delta H^{\ddagger}$ (12 kJ mol^{-1}) for the second step than that (24 kJ mol^{-1}) for the first step considered to be yielded by the higher degree of exothermic interaction of the redox pair with the water molecule in the second step than first one due to the higher positive charge, though the predominant enthalpic factor could be the exothermic dissociation enthalpy.

Although the dissociation of the complexes from the sulfonate groups should contribute positively to $\Delta S^{\ddagger}$, the reorganization

TABLE 3: Summary of the Activation Energy (E_a) and the Activation Parameters at $T = 25$ °C

redox reaction		mechanism	E_a/ kJ mol^{-1}	$\Delta G^{\ddagger a}$/ kJ mol^{-1}	$\Delta H^{\ddagger b}$/ kJ mol^{-1}	$\Delta S^{\ddagger c}$/ J K^{-1} mol^{-1}	$-T\Delta S^{\ddagger}$/ kJ mol^{-1}
first step	$Ru^{II}-R^{II}/Ru^{II}-R^{III}$	physical displacement	26 (±0.3)	79 (±0.05)	24 (±0.3)	−184 (±1.3)	55 (±0.4)
second step	$Ru^{II}-R^{III}/Ru^{III}-R^{III}$	physical displacement	14 (±1.2)	83 (±0.05)	12 (±1.2)	−234 (±4.1)	71 (±1.2)

[a] $\Delta G^{\ddagger}$ was calculated by $k = kT/h \exp(-\Delta G^{\ddagger}/RT)$, where k, *k*, *h*, and *R* are the rate constant (k_p), Boltman constant, Planck constant, and gas constant, respectively. [b] $\Delta H^{\ddagger}$ was calculated by $\Delta H^{\ddagger} = E_a - RT$ (*RT* is the zero-point energy.). [c] $\Delta S^{\ddagger}$ was calculated based on $\Delta G^{\ddagger} = \Delta H^{\ddagger} - T\Delta S^{\ddagger}$.

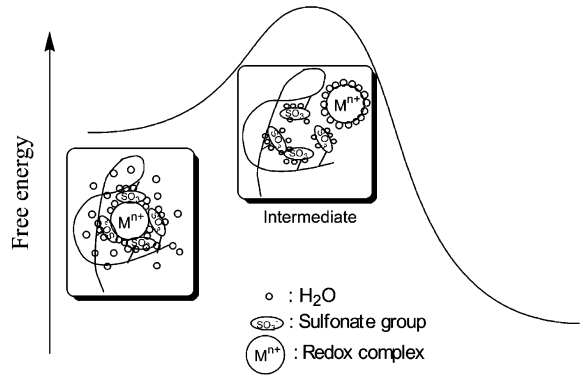

Figure 7. Imaged illustration for dissociation of a positively charged complex from the sulfonate groups of Nafion in a physical displacement mechanism. The disorder and randomness of solvents decreases in dissociation.

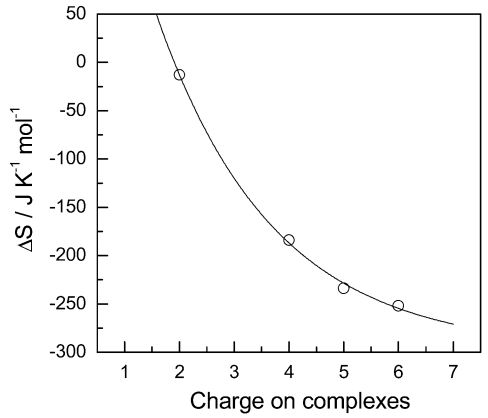

Figure 8. Plots of $\Delta S^{\ddagger}$ vs positive charge on the complex. The plots include the data of $[Ru(bpz)_3]^{2+}$ [25] and $[(NH_3)_5Ru-O-Ru(NH_3)_4-O-Ru(NH_3)_5]^{6+}$ [23] for 2+ and 6+ charges in addition to the preset data of $[Ru^{II}-Ru^{II}]^{4+}$ and $[Ru^{II}-Ru^{III}]^{5+}$ for 4+ and 5+ charges.

of the solvent as figured out in Figure 7 could produce totally the negative $\Delta S^{\ddagger}$. The lower $\Delta S^{\ddagger}$ (−234 J K^{-1} mol^{-1}) for the second step than that (−184 J K^{-1} mol^{-1}) for the first step could be explained by the higher degree of solvation required in dissociation of the $[Ru^{II}-Ru^{III}]^{5+}/[Ru^{III}-Ru^{III}]^{6+}$ redox pair from sulfonate groups of Nafion than the $[Ru^{II}-Ru^{II}]^{4+}/[Ru^{II}-Ru^{III}]^{5+}$ pair due to the highly positive charge. This could be supported by the decrease of the $\Delta S^{\ddagger}$ for physical displacement with the positive charge of complexes as shown in Figure 8, including the data reported earlier in Ru-red/Nafion ($\Delta S^{\ddagger} = -252$ J K^{-1} mol^{-1})[23] and $[Ru(bpz)_3]^{2+}$/Nafion systems ($\Delta S^{\ddagger} = -13$ J K^{-1} mol^{-1}).[25] The highly positive-charged complex is entropically unfavorable for the CT by physical displacement, presumably because of a higher degree of solvation of the complex and the sulfonate groups in their dissociation.

Conclusion

We designed a $[Ru^{II}-Ru^{II}]^{4+}$/Nafion film to study the influence of the complex charge on the CT in the film. This enabled us to compare the two successive oxidative CT processes by the $[Ru^{II}-Ru^{II}]^{4+}/[Ru^{II}-Ru^{III}]^{5+}$ (first step) and $[Ru^{II}-Ru^{III}]^{5+}/[Ru^{III}-Ru^{III}]^{6+}$ redox pair (second step) using double potential-step chronoabsorptometry (DPSCA). The predominant CT mechanism was found to be physical displacement of the complex for each step. However, the rate constant of the CT for the first step was 5.2 time higher than that for the second step at 25 °C. The CT in the second step is enthalpically favorable but entropically unfavorable compared with that for the first step. The entropic factor overcomes the corresponding enthalpic one at room temperature, providing the lower CT rate constant for the second step than that in the first step. The relation of the activation entropy for the CT by the physical displacement to the complex charge was presented, and the entropy effect on the physical displacement was first discussed. This paper reported significant features for charge and mass transport in a polymer film, providing guided thoughts for designing polymer film-modified electronic devices that will be undoubtedly extended to a wide application in the various scientific and industrial fields.

Acknowledgment. The work was partially supported by a grant from the Itoh Science Foundation.

References and Notes

(1) *Molecular design of electrode surface*; Murray, R. W., Ed.; John Wiley & Sons: New York, 1992; Vol. 22.
(2) *Electroanalytical chemistry*; Bard, A. J., Ed.; Marcel Dekker: New York, 1996; Vol. 18.
(3) Zen, J.-M.; Kumar, A. S. *Acc. Chem. Res.* **2001**, *34*, 772.
(4) Yagi, M.; Kinoshita, K.; Kaneko, M. *J. Phys. Chem.* **1996**, *100*, 11098.
(5) Yagi, M.; Kinoshita, K.; Kaneko, M. *J. Phys. Chem. B* **1997**, *101*, 3957.
(6) Yagi, M.; Kaneko, M. *Chem. Rev.* **2001**, *101*, 21.
(7) Torres, G. R.; Dupart, E.; Mingotaud, C.; Ravaine, S. *J. Phys. Chem. B* **2000**, *104*, 9487.
(8) Kaneko, M.; Woehrle, D. *Adv. Polym. Sci.* **1988**, *84*, 141.
(9) Li, W.; Osora, H.; Otero, L.; Duncan, D. C.; Fox, M. A. *J. Phys. Chem. A* **1998**, *102*, 5333.
(10) Majda, M.; Faulkner, L. R. *J. Electroanal. Chem.* **1984**, *169*, 77.
(11) Buttry, D. A.; Anson, F. C. *J. Electroanal. Chem.* **1981**, *130*, 333.
(12) Blauch, D. N.; Saveant, J. M. *J. Am. Chem. Soc.* **1992**, *114*, 3323.
(13) Blauch, D. N.; Saveant, J. M. *J. Phys. Chem.* **1993**, *97*, 6444.
(14) White, H. S.; Leddy, J.; Bard, A. J. *J. Am. Chem. Soc.* **1982**, *104*, 4811.
(15) Leddy, J.; Bard, A. J. *J. Electroanal. Chem.* **1985**, *189*, 203.
(16) Oyama, N.; Ohsaka, T.; Kaneko, M.; Sato, K.; Matsuda, H. *J. Am. Chem. Soc.* **1983**, *105*, 6003.
(17) Martin, C. R.; Rubinstein, I.; Bard, A. J. *J. Am. Chem. Soc.* **1982**, *104*, 4817.
(18) Anson, F. C.; Saveant, J. M.; Shigehara, K. *J. Phys. Chem.* **1983**, *87*, 214.
(19) Anson, F. C.; Saveant, J. M.; Shigehara, K. *J. Am. Chem. Soc.* **1983**, *105*, 1096.
(20) He, P.; Chen, X. *J. Electroanal. Chem.* **1988**, *256*, 353.
(21) Yagi, M.; Mitsumoto, T.; Kaneko, M. *J. Electroanal. Chem.* **1997**, *437*, 219.
(22) Yagi, M.; Mitsumoto, T.; Kaneko, M. *J. Electroanal. Chem.* **1998**, *448*, 131.
(23) Yagi, M.; Yamase, K.; Kaneko, M. *J. Electroanal. Chem.* **1999**, *476*, 159.
(24) Yagi, M.; Yamase, K.; Kaneko, M. *Electrochim. Acta* **2002**, *47*, 2019.

(25) Yagi, M.; Sato, T. *J. Phys. Chem. B* **2003**, *107*, 4975.
(26) Creutz, C.; Taube, H. *J. Am. Chem. Soc.* **1973**, *95*, 1086.
(27) Creutz, C.; Taube, H. *J. Am. Chem. Soc.* **1969**, *91*, 3988.
(28) It was calculated by the equation: $(1.0 \times 10^{-2}\ \mathrm{cm^3})(0.83\ \mathrm{g\ cm^{-3}})0.025/\{(2.0\ \mathrm{g\ cm^{-3}})(1.0\ \mathrm{cm^2})\} = 1.0 \times 10^{-4}$ cm.
(29) Curtis, J. C.; Sullivan, B. P.; Meyer, T. J. *Inorg. Chem.* **1983**, *22*, 224.
(30) The υ_{CT} is convenient for comparison with any case of an electrochemical reaction that cannot be analyzed by a simple diffusion process. We have adapted υ_{CT} in the CT analysis for the wide range of its application to electrochemical researches.
(31) Yagi, M.; Fukiya, H.; Kaneko, T.; Aoki, T.; Oikawa, E.; Kaneko, M. *J. Electroanal. Chem.* **2000**, *481*, 69.
(32) The k_p obtained is a phenomenological value including equilibria, the reorganization of the solvent and counterion migration involved in CT rather than a real rate constant, so these values should be sensitive to the solvent and a supporting electrolyte. However, in the present CT system, we did not observe any distinguishable changes in CT kinetics for both the 1st and 2nd steps when $NaNO_3$, K_2SO_4, and $NaClO_4$ were used in stead of KNO_3. This result shows that counterion migration does not influence significantly phenomenological CT under the conditions applied in the present system though it should be involved in the CT.